Research Square

Preprints are preliminary reports that have not undergone peer review.
They should not be considered conclusive, used to inform clinical practice,
or referenced by the media as validated information.

m6A-modified lncRNA MIR210HG promotes endometrial cancer by directly interacting with CPSF1

Jiahua Chen
Second Affiliated Hospital of Anhui Medical University
Haiqing Zhu
Second Affiliated Hospital of Anhui Medical University
Jing Zhang
Second Affiliated Hospital of Anhui Medical University
Xiaojing Liu
Second Affiliated Hospital of Anhui Medical University
Yuan Fang
Second Affiliated Hospital of Anhui Medical University
Junhui Zhang
Second Affiliated Hospital of Anhui Medical University
Lei Zhan
499329901@qq.com

First Affiliated Hospital of Anhui Medical University

Research Article

Keywords: endometrial cancer, m6A modification, long non-coding RNA, MIR210HG, METTL3, cancer progression

Posted Date: November 23rd, 2026

DOI: https://doi.org/10.21203/rs.3.rs-11187569/v1

License: This work is licensed under a Creative Commons Attribution 4.0 International License.
Read Full License

Additional Declarations:
No competing interests reported.

Tables are available in the Supplementary Files section

m6A-modified lncRNA MIR210HG promotes endometrial cancer by directly interacting with CPSF1

Jiahua Chen[2*], Haiqing Zhu[2*], Jing Zhang[2], Xiaojing Liu[2], Yuan Fang[2], Junhui Zhang[2†] and Lei Zhan[1†]

[1]Department of Obstetrics and Gynecology, The First Affiliated Hospital of Anhui Medical University, No 218 Jixi Road, Hefei, 230022, Anhui, China

[2] Department of Obstetrics and Gynecology, The Second Affiliated Hospital of Anhui Medical University, No 678 Furong Road, Hefei, 230601, Anhui, China

†**Correspondence**:

Junhui Zhang

2410392149@qq.com

Lei Zhan

499329901@qq.com

Full list of author information is available at the end of the article

[*]Jiahua Chen and Haiqing Zhu contributed equally to this work and share first authorship.

Keywords: endometrial cancer; m6A modification; long non-coding RNA; MIR210HG; METTL3; cancer progression

Abstract

Numerous studies have shown that aberrant expression of long non-coding RNAs (lncRNAs) is associated with tumors and has potential as a therapeutic target. The role of the lncRNA MIR210 Host Gene (MIR210HG) in endometrial cancer (EC) needs to be studied in greater depth. In this study we report for the first time that MIR210HG is negatively regulated by methyltransferase like 3 (METTL3). Functional assays showed that overexpression of MIR210HG was able to attenuate the tumor-suppressive effects of METTL3. MIR210HG was further found to increase cleavage and polyadenylation specific factor 1 (CPSF1) expression by Mass Spectrometer (MS) and western blot. Mechanistically, METTL3 regulates the RNA stability of MIR210HG in an m6A-dependent manner to reduce its expression, and MIR210HG promotes malignant biological behaviors by enhancing CPSF1 expression at the protein level through direct binding to CPSF1. Our study provides a more solid basis for MIR210HG as a new tumor marker and therapeutic target.

Introduction

LncRNAs are a class of RNA molecules exceeding 200 nucleotides in length, with a minority capable of encoding short peptides[1]. They are ubiquitously present in eukaryotes. Through transcriptional and post-transcriptional mechanisms, lncRNAs primarily drive malignant behaviors in tumors including proliferation, migration, and invasion[2]. LncRNA MIR210HG, a 567-nucleotide transcript located at chromosome 21q13.3, serves as the host gene for miR-210[3]. Substantial evidence indicates its critical involvement in tumorigenesis and cancer progression. In colorectal cancer, MIR210HG promotes tumor cell proliferation by binding PCBP1 to inhibit ferroptosis[4].In gastric cancer, c-MYC activates MIR210HG expression to synergistically promote malignant progression[5].MIR210HG further forms a

positive feedback loop with HIF-1α to drive proliferation, migration, and invasion in cervical cancer[6]. However, the functional roles and molecular mechanisms of MIR210HG in EC remain poorly understood.

N6-methyladenosine (m6A) represents the predominant RNA modification in eukaryotic cells[7]. Dysregulation of m6A regulatory factors is closely associated with tumorigenesis across various cancers[7]. Substantial evidence demonstrates that aberrant expression of m6A modifiers critically influences multiple oncogenic processes[8]. Emerging research further reveals that m6A regulators modulate all non-coding RNAs, including lncRNAs, thereby contributing to diverse pathological developments[9]. As the sole catalytic subunit of the m6A methyltransferase complex, METTL3 plays a pivotal role in mediating m6A modifications on lncRNAs[10,11]. Studies demonstrate that METTL3 accelerates cervical cancer progression by enhancing FOXD2-AS1 expression through m6A-dependent mechanisms[12]. Recent work indicates METTL3 participates in endometrial carcinogenesis via regulation of the AKT signaling pathway[13]. However, the regulatory interplay between METTL3 and lncRNAs in EC remains largely unexplored.

Cleavage and polyadenylation specificity factor 1 (CPSF1), the largest subunit of the cleavage and polyadenylation specificity factor complex, recognizes the canonical AAUAAA polyadenylation signal in precursor messenger RNA (pre-mRNA). It facilitates RNA cleavage and poly(A) tail synthesis by serving as a scaffold for the assembly of the 3'-end processing machinery[14].Numerous studies have established that CPSF1 contributes to tumor progression through diverse mechanisms, including modulation of glycolytic pathways, chemoresistance, and post-translational modifications[15–17].

Here, we identified a METTL3/MIR210HG/CPSF1 regulatory axis in EC. METTL3 negatively regulates MIR210HG and reduces its RNA stability in an m6A-dependent manner. Overexpression of MIR210HG attenuates the tumor-suppressive effects of METTL3 in EC. MIR210HG directly binds

CPSF1 protein to execute pro-oncogenic functions. Our findings validate m6A-modified lncRNA MIR210HG as a novel biomarker and therapeutic target in EC.

Materials and methods

Tissue samples

Tissue samples were obtained from EC patients undergoing surgical resection at the Department of Obstetrics and Gynecology, The Second Affiliated Hospital of Anhui Medical University (Hefei, China), following written informed consent. The cohort comprised 8 EC and 8 matched normal tissues, snap-frozen and stored at −80°C. This study received approval from the Hospital's Research Ethics Committee.

Cell lines and cell culture

HEC-1B and Ishikawa human endometrial cancer cell lines were purchased from ATCC and ECACC, respectively. HEC-1B cells were cultured in RPMI-1640 medium, whereas Ishikawa cells were maintained in DMEM (Bio-channel, China), both supplemented with 10% FBS (Gibco, USA). All cells were grown at 37°C in a humidified incubator with 5% CO_2. Both cell lines were confirmed to be mycoplasma-free and were used within three years of authentication.

Bioinformatics analysis

Gene expression profiles of EC were retrieved from The Cancer Genome Atlas (TCGA; https://portal.gdc.cancer.gov). Differentially expressed genes in TCGA-UCEC were identified using the 'edgeR' package. Heatmap, volcano plot, and pan-cancer plots were generated with the 'ggplot2' package. Pearson correlation analysis between METTL3 and lncRNA MIR210HG was performed via GEPIA.

Transfection of cells

The pcDNA3.1-MIR210HG overexpression plasmid, pcDNA3.1-NC control vector, si-MIR210HG, and si-NC were commercially supplied by GenePharma (Shanghai, China). Transfections were carried out with jetPRIME® reagent (Polyplus, France) in accordance with the manufacturer's instructions at the prescribed transfection concentration. Sequences of primers used for siRNA are listed in Table 1.

Lentivirus construction and infection

GenePharma (Shanghai, China) supplied lentiviral constructs for METTL3 overexpression and knock-down, each carrying GFP and puromycin resistance. Empty vectors served as controls. Stable cell lines were established via puromycin selection (2 μg/mL), and METTL3 expression was confirmed by qRT-PCR and western blot analysis. Sequences of primers used for shRNA are listed in Table 1.

Western blot assay

Western blot assay was performed as previously described[18]. GAPDH served as the loading control. Detailed specifications for primary antibodies are provided in Table 2.

RNA extraction and quantitative reverse transcription polymerase chain reaction (qRT-PCR)

According to the manufacturer's protocols, total RNA was extracted from tissues and cells using the HyperPure RNA Isolation Kit (NovaBio, China) and reverse-transcribed into cDNA with HyperScript III RT SuperMix (NovaBio, China). Primers specific for METTL3, MIR210HG, β-actin, U6, MBNL1-AS1, RHPN1-AS1, DARS-AS1, and CPSF1 were provided by NovaBio (Shanghai, China). The expression levels of target genes were analyzed by qRT-PCR, and relative expression was determined using the 2^−ΔΔCt method with β-actin serving as the endogenous control.The primer sequences are listed in Table 3.

Cell proliferation assay

Ishikawa and HEC-1B cells were seeded into 96-well plates and maintained at 37°C in an atmosphere containing 5% CO_2. After incubation for 24, 48, and 72 h, cell proliferation was determined using the CCK-8 assay (Dojindo, Japan). Briefly, 10 μL of CCK-8 reagent was added to each well and incubated for an additional 2 h. Absorbance was measured at 450 nm using a microplate reader, and the results were used to evaluate cell growth.

Transwell assay

To investigate the migration and invasion ability of EC cells, 8-mm pore size culture inserts (Transwell, Corning, USA) were purchased. For invasion assay, Matrigel (Corning) was diluted by serum-free medium at a ratio of 1:8 to pretreat at the upper chamber and 1×10^5 cells were seeded in each upper chamber. Then, 700 μL of 10% FBS-containing medium was added to the lower chamber. After a 24h-culter period (migration) or 48h-culter period (invasion), cells were fixed with 4% Paraformaldehyde and dyed with 0.1% crystal violet. Cells in upper chambers were photographed by microscope (Olmypus, Japan) and counted by image J.

Colony formation assay

EC cells (1000 cells/well or 500 cells/well) were seeded in 6-well plates or 12-well plates in triplicate. After 14 days incubation, cells were fixed with 4% Paraformaldehyde at room temperature and dyed with 0.1% crystal violet for 30 min.

Subcellular fraction assay

The nucleus and cytoplasm of the cell were separated by PARISTM Kit (Invitrogen, USA), and the RNA of these two parts was extracted for qRT-PCR assay. The expression of target genes and internal reference genes in the cytoplasm and nucleus were detected as a percentage of the total cellular expression. The primer sequences are listed in Table 3.

m6A RNA immunoprecipitation assay

To assess m6A methylation of MIR210HG, an EpiMark® N6-Methyladenosine Enrichment Kit (New

England Biolabs, UK) was utilized. The enriched RNA was isolated after the immunoprecipitation procedure and subsequently quantified by qRT-PCR. Relative m6A enrichment levels were normalized against input RNA controls.

RNA pull-down assay and MS

The RNA pull-down kit (BersinBio, China) was purchased to detect lncRNA MIR210HG binding proteins. The biotin-labeled probe of MIR210HG and LacZ was synthesized by BersinBio. The sample preparation was according to the manufacturer's instruction and verified by MS and western blot assay.

RNA Immunoprecipitation (RIP) assay

The RIP assay was performed following the instruction of RIP kit (BersinBio, China). Total 2×10^7 cells were lysed and incubated with primary antibody at 4℃ overnight. The primary antibody-lysis mix incubated with beads at 4℃ for 1h. Then RNA was extracted, reverse transcribed and analyzed with qRT-PCR

RNA stability assay

Actinomycin D (AD) at 5ug/ml was added to the cells for incubation and RNA was extracted at 0 h, 3 h and 6 h for qRT-PCR. Gene expression was normalized to lncRNA MIR210HG levels at 0 h.

Statistics

Statistical calculations and figure preparation were carried out using GraphPad Prism 9.0. An unpaired Student's *t*-test was applied for comparisons between two groups, while one-way ANOVA followed by Tukey's post hoc test was used for analyses involving more than two groups. Results are presented as mean ± SD, and statistical significance was established at $P < 0.05$.

Results

METTL3 exerts tumor-suppressive effects *in vitro*

First, to investigate the biological functions of METTL3 in EC cell lines, we established stable transfectants via lentiviral transduction: Ishikawa/HEC-1B-NC, Ishikawa/HEC-1B-METTL3, Ishikawa/HEC-1B-shNC, and Ishikawa/HEC-1B-shMETTL3. Transfection efficiency was validated by both Western

blotting (Fig. 1A, B). Cell proliferation was subsequently assessed using CCK-8 assays. Results demonstrated significantly inhibited proliferation in the METTL3 group compared to NC controls, whereas shMETTL3 transfection produced the opposite effect (Fig. 1C-F). Consistent trends were observed in Transwell assays: METTL3 overexpression suppressed migration and invasion capabilities in both Ishikawa and HEC-1B cell lines (Fig. 1G, H).

Regulatory relationship between lncRNA MIR210HG and METTL3

To identify METTL3-regulated downstream lncRNAs, we first analyzed the UCEC-TCGA transcriptomic dataset (Tumor=543, Normal=35), identifying differentially expressed lncRNAs visualized through heatmap and volcano plot (Fig. 2A, B). Candidate m6A-modified lncRNAs were predicted using SRAMP, yielding four targets (MBNL1-AS1, RHPN1-AS1, MIR210HG, and DARS-AS1). Validation in Ishikawa cell lines (Ishikawa-NC, Ishikawa-METTL3, Ishikawa-shNC, Ishikawa-shMETTL3) confirmed METTL3-mediated negative regulation of MIR210HG (Fig. 2C).

Tumor-Associated Characteristics of lncRNA MIR210HG

Integrated TCGA-GTEx analysis revealed elevated MIR210HG expression across multiple tumor types (Fig. 3A). Further examination of TCGA-UCEC-GTEx data (Tumor=174, Normal=91) demonstrated significant MIR210HG upregulation in EC (Fig. 2E). qRT-PCR validation in 8 normal endometrial and 8 EC specimens confirmed this overexpression pattern (Fig. 3B). Given the functional significance of subcellular localization, nuclear-cytoplasmic fractionation assays showed MIR210HG distribution in both compartments, with predominant nuclear enrichment (Fig. 3C).

METTL3 promotes degradation of MIR210HG in an m6A-dependent manner

To determine whether METTL3 regulates lncRNA MIR210HG via m6A-dependent mechanisms, we first identified two potential m6A modification sites at positions 476 and 482 of MIR210HG using SRAMP. Secondary structure visualizations were generated based on these predictions (Fig. 4A, B). Correlation analysis of TCGA-UCEC data via GEPIA revealed a significant negative association between METTL3 and MIR210HG RNA levels, consistent with our experimental findings (Fig. 4C). MeRIP-qPCR assays demonstrated significantly reduced m6A enrichment on MIR210HG in shMETTL3 groups

compared to shNC controls (Fig. 4D). RNA stability assays further showed decreased MIR210HG stability in METTL3 cells versus NC groups (Fig. 4E).

MIR210HG exerts pro-oncogenic functions in EC cell lines

To investigate the biological functions of lncRNA MIR210HG in Ishikawa and HEC-1B cells, we established overexpression and knockdown models using plasmid transfection and short interfering RNA (siRNA), respectively. Transfection efficiency was validated by qRT-PCR (Fig. 5A). Proliferation, migration, and invasion capabilities were subsequently assessed through CCK-8, Transwell, and colony formation assays. Compared to the empty vector control, MIR210HG overexpression significantly enhanced malignant phenotypes. Conversely, siRNA-mediated knockdown of MIR210HG (si-MIR210HG) suppressed proliferative, migratory, and invasive capacities relative to the si-NC group (Fig. 5B-E).

MIR210HG attenuates the tumor-suppressive effects of METTL3 in EC

Prior findings established METTL3 as a tumor suppressor and MIR210HG as an oncogenic driver in EC. To determine whether MIR210HG serves as a critical downstream effector of METTL3-mediated tumor suppression, we generated four experimental groups in HEC-1B and Ishikawa cell lines: NC, METTL3 overexpression, METTL3 & MIR210HG co-overexpression, and MIR210HG overexpression. Transfection efficiency was first validated by qRT-PCR (Fig. 6A). CCK-8 assays demonstrated that MIR210HG overexpression attenuated the anti-proliferative effects of METTL3 (Fig. 6B). Consistent trends emerged in Transwell migration/invasion and colony formation: MIR210HG co-expression counteracted METTL3-induced suppression of migratory capacity, invasive potential, and colony formation (Fig. 6C-E).

MIR210HG directly binds with CPSF1 and promotes its protein expression

Emerging research elucidates the biofunction of lncRNAs, which is tied to their subcellular localization[19]. Our previous experiments showed that MIR210HG is mainly expressed in the cell nucleus. Recent studies have increasingly shown that lncRNAs can directly interact with proteins and thus participate in post-transcriptional, translational, and post-translational regulation[20,21]. We therefore performed RNA pull-down and MS to identify proteins interacting with MIR210HG. Results demonstrated significant enrichment of CPSF1, indicating an interaction between CPSF1 and MIR210HG (Fig. 7A).

The peptide mass fingerprinting of CPSF1 was displayed in Fig. 7B. RIP assays using anti-CPSF1 antibody were performed to validate the interaction between MIR210HG and CPSF1 in Ishikawa and HEC-1B EC cell lines (Fig. 7C). Subsequently, when investigating whether MIR210HG regulates CPSF1 expression, we observed that MIR210HG overexpression did not significantly alter CPSF1 mRNA levels, while it enhanced CPSF1 protein levels (Fig. 7D, E).

Discussion

In this study, we demonstrate that METTL3 suppresses the MIR210HG landscape by compromising its transcript half-life in an m6A-dependent manner. Beyond its role as a target of METTL3, MIR210HG actively modulates the proteomic profile by directly interacting with CPSF1. This binding event enhances the abundance of the CPSF1 protein, thereby empowering the cells with increased proliferative and migratory capacities. These findings highlight a novel METTL3/MIR210HG/CPSF1 signaling axis in cancer progression (Fig.8).

Accumulating evidence suggests that m6A modification plays a pivotal role in the development and progression of EC[22,23]. METTL3 acts as a core RNA methyltransferase that serves as a "writer" to catalyze m6A modification[24]. Our study reveals that METTL3 significantly inhibits malignant biological behaviors in EC cells, specifically suppressing migration and proliferation. These findings support the role of METTL3 as a tumor suppressor, which is consistent with previous reports[13]. However, the role of METTL3 in EC is remarkably complex. Contrary to our findings, some studies report high METTL3 expression in drug-resistant cells, where it promotes immune evasion[25]. We hypothesize that this phenotypic polarization may stem from differences in cellular functional states and genetic backgrounds.

Epigenetic regulations such as histone remodeling and DNA/RNA methylation, frequently underlie the aberrant expression of lncRNAs[26,27]. Recent studies show that m6A modification influences lncRNA stability. This process is essential for the regulatory impact of lncRNAs on cellular processes[28,29]. Our data reveal a METTL3-dependent m6A modification on MIR210HG. Such modification influences transcript stability to regulate the progression of EC. Typically, m6A modified RNAs are recognized by "reader" proteins, which in turn modulate transcript stability. In the present study, the specific mechanisms underlying this process remain to be further elucidated. In subsequent experiments, we further explored the METTL3/MIR210HG axis in EC. We found that MIR210HG overexpression

attenuated the tumor-suppressive effects of METTL3, suggesting that MIR210HG is a key downstream target of METTL3.

The functional roles of lncRNAs are closely dictated by their subcellular localization. While nuclear lncRNAs typically modulate gene expression at the transcriptional level by interacting with DNA or transcription factors, those in the cytoplasm primarily govern post-transcriptional processes, such as serving as competing endogenous RNAs (ceRNAs) to sequester miRNAs or directly regulating mRNA stability. In this study, nuclear-cytoplasmic fractionation assays revealed that MIR210HG is present in both compartments but is predominantly enriched in the nuclear fraction. Consequently, we hypothesize that MIR210HG primarily functions as a transcriptional regulator in the progression of EC. RNA pull-down assays further identified CPSF1 as a direct binding partner of MIR210HG. Intriguingly, we observed that MIR210HG promotes the accumulation of CPSF1 protein without altering its mRNA levels. This pattern of regulation indicates that the lncRNA may enhance the stability of the CPSF1 protein or facilitate its translation. The hypothesis is still needed further experimental validation. In recent years, a growing body of evidence has characterized CPSF1 as a molecular 'accelerator' or key regulator across diverse malignancies[15–17]. However, the specific role of CPSF1 in EC remains poorly understood, and further experimental investigation is urgently required to elucidate its function.

Conclusion

In summary, we demonstrate that METTL3 reduces MIR210HG expression by decreasing its RNA stability through m6A-dependent mechanisms. Conversely, MIR210HG enhances CPSF1 protein abundance via direct binding, thereby promoting malignant phenotypes.

Acknowledgements

We are grateful to all women who consented and donated samples for this study.

Authors' contributions

Jiahua Chen and Haiqing Zhu conducted the study and wrote the manuscript. Haiqing Zhu, Jing Zhang, and Xiaojing Liu recruited patients and collected samples. Jiahua Chen, Haiqing Zhu, and Yuan Fang performed the experiments. Jiahua Chen and Haiqing Zhu performed data analyses. Lei Zhan and Junhui

Zhang designed and supervised the study. All authors reviewed and agreed to the final version of the manuscript.

Funding

This study was supported by the National Nature Science Foundation of China (grant 81802586), the Open Research Project of Engineering Research Center of Biopreservation and Artificial Organs, Ministry of Educatior (ERC-2025-05), and the Open Research Project of Anhui Province Key Laboratory of Reproductive Disorders and Obstetrics and Gynaecology Diseases (RDOGD-2025-11).

Data accessibility

The datasets generated and analyzed during this study are derived from publicly available resources, including the TCGA and GEPIA databases. The datasets generated or analyzed during this study are available from the corresponding author on reasonable request.

Ethics approval and consent to participate

This study was approved by the Institutional Review Board of Anhui Medical University (No: 20180023). A written informed consent was obtained from all patients prior to sample collection and storage.

Competing interests

The authors declare that they have no known competing financial interests or personal relationships that could have appeared to influence the work reported in this paper.

References

[1] Nojima T, Proudfoot NJ. Mechanisms of lncRNA biogenesis as revealed by nascent transcriptomics. Nat Rev Mol Cell Biol 2022;23:389–406. https://doi.org/10.1038/s41580-021-00447-6.

[2] Nadhan R, Isidoro C, Song YS, Dhanasekaran DN. LncRNAs and the cancer epigenome: Mechanisms and therapeutic potential. Cancer Lett 2024;605:217297. https://doi.org/10.1016/j.canlet.2024.217297.

[3] Voellenkle C, Garcia-Manteiga JM, Pedrotti S, Perfetti A, De Toma I, Da Silva D, et al. Implication of long noncoding RNAs in the endothelial cell response to hypoxia revealed by RNA-sequencing. Sci Rep 2016;6:24141. https://doi.org/10.1038/srep24141.

[4] Wang X-Q, Fan A-Q, Hong L. LncRNA MIR210HG promotes the proliferation of colon cancer cells by inhibiting ferroptosis through binding to PCBP1. Sci Rep 2025;15:871. https://doi.org/10.1038/s41598-025-85321-7.

[5] Li Z-Y, Xie Y, Deng M, Zhu L, Wu X, Li G, et al. c-myc-activated intronic miR-210 and lncRNA

MIR210HG synergistically promote the metastasis of gastric cancer. Cancer Lett 2022;526:322–34. https://doi.org/10.1016/j.canlet.2021.11.006.

[6] Hu X-L, Huang X-T, Zhang J-N, Liu J, Wen L-J, Xu X, et al. Long noncoding RNA MIR210HG is induced by hypoxia-inducible factor 1α and promotes cervical cancer progression. Am J Cancer Res 2022;12:2783–97.

[7] Jiang X, Liu B, Nie Z, Duan L, Xiong Q, Jin Z, et al. The role of m6A modification in the biological functions and diseases. Signal Transduct Target Ther 2021;6:74. https://doi.org/10.1038/s41392-020-00450-x.

[8] Fang Z, Mei W, Qu C, Lu J, Shang L, Cao F, et al. Role of m6A writers, erasers and readers in cancer. Exp Hematol Oncol 2022;11:45. https://doi.org/10.1186/s40164-022-00298-7.

[9] Yi Y-C, Chen X-Y, Zhang J, Zhu J-S. Novel insights into the interplay between m6A modification and noncoding RNAs in cancer. Mol Cancer 2020;19:121. https://doi.org/10.1186/s12943-020-01233-2.

[10] Jiang T, Qi J, Xue Z, Liu B, Liu J, Hu Q, et al. The m6A modification mediated-lncRNA POU6F2-AS1 reprograms fatty acid metabolism and facilitates the growth of colorectal cancer via upregulation of FASN. Mol Cancer 2024;23:55. https://doi.org/10.1186/s12943-024-01962-8.

[11] Xi Q, Yang G, He X, Zhuang H, Li L, Lin B, et al. M6A-mediated upregulation of lncRNA TUG1 in liver cancer cells regulates the antitumor response of CD8+ T cells and phagocytosis of macrophages. Adv Sci 2024;11:2400695. https://doi.org/10.1002/advs.202400695.

[12] Ji F, Lu Y, Chen S, Lin X, Yu Y, Zhu Y, et al. m6A methyltransferase METTL3-mediated lncRNA FOXD2-AS1 promotes the tumorigenesis of cervical cancer. Mol Ther - Oncolytics 2021;22:574–81. https://doi.org/10.1016/j.omto.2021.07.004.

[13] Liu J, Eckert MA, Harada BT, Liu S-M, Lu Z, Yu K, et al. m6A mRNA methylation regulates AKT activity to promote the proliferation and tumorigenicity of endometrial cancer. Nat Cell Biol 2018;20:1074–83. https://doi.org/10.1038/s41556-018-0174-4.

[14] Murthy KG, Manley JL. The 160-kD subunit of human cleavage-polyadenylation specificity factor coordinates pre-mRNA 3'-end formation. Genes Dev 1995;9:2672–83. https://doi.org/10.1101/gad.9.21.2672.

[15] Tietz KT, McCluskey BM, Miller CR, Li Y, Munro SA, Dehm SM. CPSF1 inhibition promotes widespread use of intergenic polyadenylation sites and impairs glycolysis in prostate cancer cells. Cell Rep 2025;44:115211. https://doi.org/10.1016/j.celrep.2024.115211.

[16] Guo Q, Wang H, Duan J, Luo W, Zhao R, Shen Y, et al. An alternatively spliced p62 isoform confers resistance to chemotherapy in breast cancer. Cancer Res 2022;82:4001–15. https://doi.org/10.1158/0008-5472.CAN-22-0909.

[17] Mayro B, Hoj JP, Cerda-Smith CG, Hutchinson HM, Caminear MW, Thrash HL, et al. ABL kinases regulate the stabilization of HIF-1α and MYC through CPSF1. Proc Natl Acad Sci U S A n.d.;120:e2210418120. https://doi.org/10.1073/pnas.2210418120.

[18] Zhan L, Zhang J, Zhang J, Liu X, Zhu S, Shi Y, et al. LC3 and NLRC5 interaction inhibits NLRC5-mediated MHC class I antigen presentation pathway in endometrial cancer. Cancer Lett 2022;529:37–52. https://doi.org/10.1016/j.canlet.2021.12.031.

[19] Statello L, Guo C-J, Chen L-L, Huarte M. Gene regulation by long non-coding RNAs and its biological functions. Nat Rev Mol Cell Biol 2021;22:96–118. https://doi.org/10.1038/s41580-020-00315-9.

[20] Mahajan A, Chandran S, Kumar A, Chen L, Dhillon NK. LncRNA-536 and RNA-binding protein

RBM25 interactions in pulmonary artery smooth muscle cells: Implications in pulmonary hypertension. Arterioscler Thromb Vasc Biol 2025. https://doi.org/10.1161/ATVBAHA.125.322734.

[21] Du H, Zhao Y, Wen J, Dai B, Hu G, Zhou Y, et al. LncRNA DCRT protects against dilated cardiomyopathy by preventing NDUFS2 alternative splicing by binding to PTBP1. Circulation 2024;150:1030–49. https://doi.org/10.1161/CIRCULATIONAHA.123.067861.

[22] Wang B, Wang Y, Wang W, Wang Z, Zhang Y, Pan X, et al. WTAP/IGF2BP3 mediated m6A modification of the EGR1/PTEN axis regulates the malignant phenotypes of endometrial cancer stem cells. J Exp Clin Cancer Res CR 2024;43:204. https://doi.org/10.1186/s13046-024-03120-w.

[23] Ke J, Gao T, Shen Z, Li M, Zhang T, Wu D. Mechanism of LncRNA NORAD regulating ferroptosis in endometrial cancer cells by modifying GPX4 through FTO-mediated m6A methylation. Cell Mol LIFE Sci CMLS 2025;82:364. https://doi.org/10.1007/s00018-025-05855-x.

[24] Chen J, Guo B, Liu X, Zhang J, Zhang J, Fang Y, et al. Roles of N6-methyladenosine (m6A) modifications in gynecologic cancers: Mechanisms and therapeutic targeting. Exp Hematol Oncol 2022;11:98. https://doi.org/10.1186/s40164-022-00357-z.

[25] Hao M, Li T, Xiao L, Liu Y. METTL3-induced FGD5-AS1 contributes to the tumorigenesis and PD-1/PD-L1 checkpoint to enhance the resistance to paclitaxel of endometrial carcinoma. J Cell Mol Med 2024;28:e17971. https://doi.org/10.1111/jcmm.17971.

[26] Yamazaki K, Mizukami H, Yamada T, Hara Y, Tamba H, Tatara Y, et al. MEG3 promoter methylation and F11 receptor (F11R) overexpression define a high-risk subtype of diabetic pancreatic cancer. Mod Pathol Off J U S Can Acad Pathol Inc 2026;39:100953. https://doi.org/10.1016/j.modpat.2025.100953.

[27] Lang C, Mu X, Chen K, Wang X, Rong Y, Wang J, et al. Epigenetic activation of CCDC183-AS1 promotes osteoclastogenesis and prostate cancer bone metastasis through the FUBP1/LIGHT axis. Adv Sci 2025;12:e13288. https://doi.org/10.1002/advs.202413288.

[28] Wei G, Coker H, Rodermund L, Almeida M, Roach HL, Nesterova TB, et al. m6A and the NEXT complex direct xist RNA turnover and X-inactivation dynamics. Nat Struct Mol Biol 2025;32:2242–51. https://doi.org/10.1038/s41594-025-01663-w.

[29] Wu O, Jin Y, Zhang Z, Zhou H, Xu W, Chen L, et al. KMT2A regulates the autophagy-GATA4 axis through METTL3-mediated m6A modification of ATG4a to promote NPCs senescence and IVDD progression. Bone Res 2024;12:67. https://doi.org/10.1038/s41413-024-00373-1.

Figure legends

Fig.1 METTL3 exerts tumor-suppressive effects *in vitro*. A-B Western blotting analysis of METTL3 expression in stable transfectants: Ishikawa/HEC-1B-NC, Ishikawa/HEC-1B-METTL3, Ishikawa/HEC-1B-shNC, and Ishikawa/HEC-1B-shMETTL3. C-F CCK-8 assays evaluating proliferation capacity across transfected cell groups. G-H Transwell migration assays assessing migratory capabilities. E Transwell invasion assays quantifying invasive potential. **P* < 0.05; ***P* < 0.01; ****P* < 0.001.

Fig. 2 Regulatory relationship between lncRNA MIR210HG and METTL3. A Heatmap of differentially expressed lncRNAs in normal (n=35) vs. tumor (n=543) samples. B Volcano plot of differential lncRNA expression in normal (n=35) vs. tumor (n=543) groups. C qRT-PCR analysis of candidate lncRNAs in Ishikawa-NC, Ishikawa-METTL3, Ishikawa-shNC, and Ishikawa-shMETTL3. **P* < 0.05; ***P* < 0.01; ****P* < 0.001; ns, not significant.

Fig.3 Tumor-Associated Characteristics of lncRNA MIR210HG.A Pan-cancer analysis of MIR210HG expression across tumor type. B Box plot showing MIR210HG expression in EC (Tumor=174, Normal=91). C qRT-PCR quantification of MIR210HG in normal endometrial (n=8) vs. EC (n=8) specimens. D Subcellular distribution of MIR210HG by nuclear-cytoplasmic fractionation. **P* < 0.05; ****P* < 0.001; ns, not significant.

Fig.4 METTL3 promotes degradation of MIR210HG in an m6A-dependent manner. A SRAMP prediction of m6A modification sites on MIR210HG. B Schematic representation of MIR210HG secondary structure at m6A modification sites. C Correlation analysis between METTL3 and MIR210HG in TCGA database. D m6A enrichment levels of MIR210HG measured by MeRIP-qPCR. E RNA stability assessment of MIR210HG. **P* < 0.05; ***P* < 0.01.

Fig.5 MIR210HG exerts pro-oncogenic functions in EC cell lines. A qRT-PCR validation of MIR210HG transfection efficiency in Ishikawa and HEC-1B cells. B CCK-8 proliferation assays in MIR210HG-transfected EC cells. C Transwell migration analysis in MIR210HG-transfected EC cells. D Transwell invasion assessment in MIR210HG-transfected EC cells. E Colony formation assay in EC cells following MIR210HG manipulation. **P* < 0.05; ***P* < 0.01; ****P* < 0.001.

Fig.6 MIR210HG attenuates the tumor-suppressive effects of METTL3 in EC. A qRT-PCR anal ysis of MIR210HG and METTL3 expression in Ishikawa/HEC-1B cell groups. B. CCK8 was u sed to measure proliferation of Ishikawa and HEC-1B EC cells transduced with empty vector c ontrol, LV- METTL3+MIR210HG plasmid, and MIR210HG plasmid. C, D Transwell migration and invasion assays in Ishikawa/HEC-1B cells with NC, METTL3, METTL3+MIR210HG, MIR 210HG. E Colony formation assay of METTL3 or/and MIR210HG-transfected Ishikawa and he c01b EC cells. **P* < 0.05; ***P* < 0.01; ****P* < 0.001; ns, not significant.

Fig.7 MIR210HG directly binds with CPSF1 and promotes its protein expression. A. RNA pull-down assays were conducted using biotinylated antisense MIR210HG or LacZ probes. The associated proteins were separated by SDS-PAGE and subsequently visualized by silver staining. B. CPSF1 was identified among the proteins enriched in the RNA pull-down complexes by MS analysis. C. RIP assays were performed in Ishikawa and HEC-1B endometrial cancer cells using an anti-CPSF1 antibody, followed by RT-qPCR detection of MIR210HG enrichment in the immunoprecipitated fractions. D. CPSF1 protein expression was examined by western blotting in Ishikawa and HEC-1B cells transfected with either the MIR210HG overexpression vector or the corresponding empty vector. E. Relative CPSF1 mRNA levels were determined by RT-qPCR in Ishikawa and HEC-1B cells following transfection with the MIR210HG overexpression plasmid or control vector. **P* < 0.05; ***P* < 0.01; ****P* < 0.001; ns, not significant.

Fig.8 Schematic diagram. Schematic diagram for the mechanisms of METTL3/MIR210HG/CPSF 1 axis in EC.

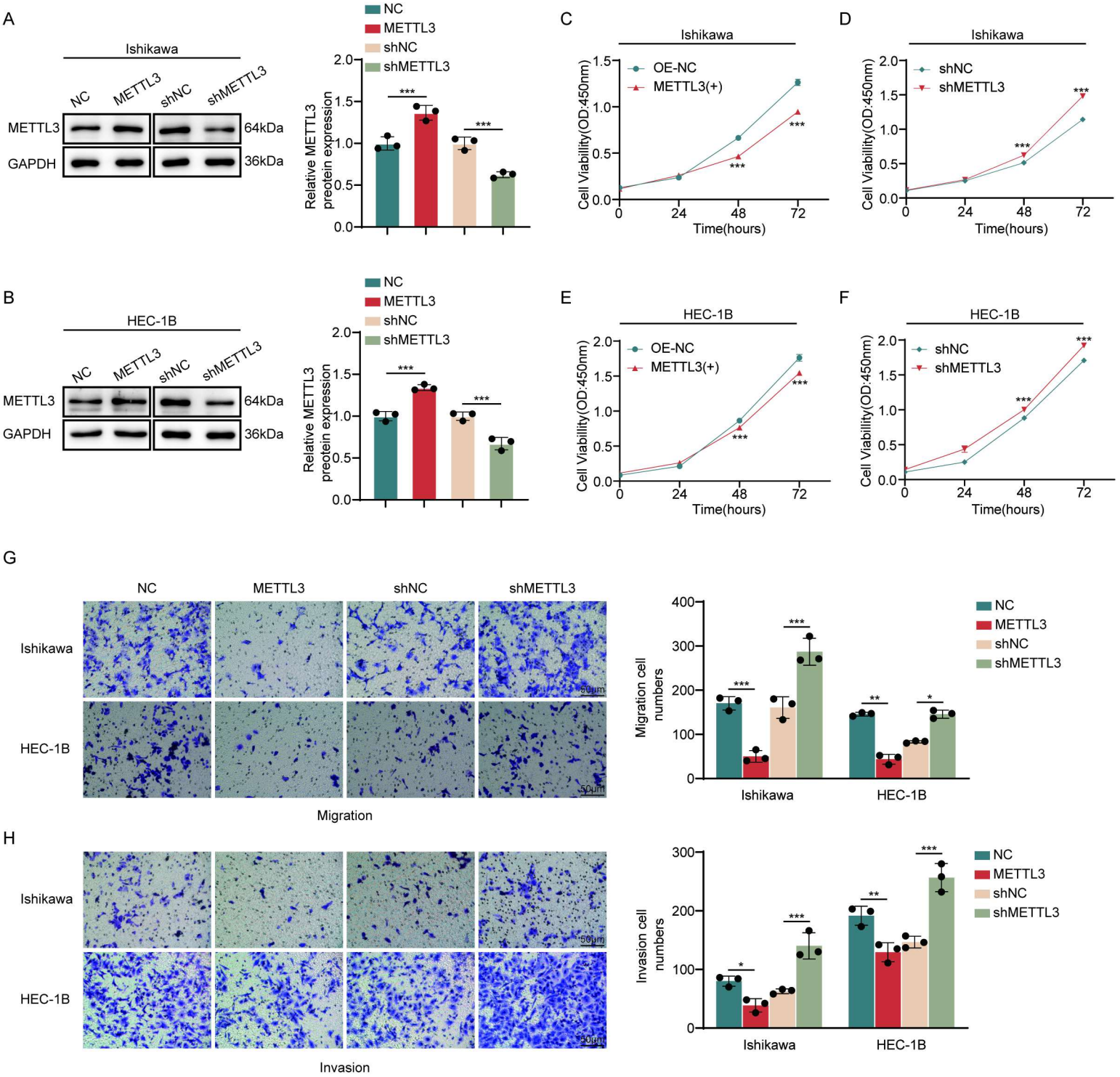
A
Ishikawa
NC
METTL3
shNC
shMETTL3
METTL3
GAPDH
64kDa
36kDa
NC
METTL3
shNC
shMETTL3
Relative METTL3 preotein expression
B
HEC-1B
C
Ishikawa
OE-NC
METTL3(+)
Cell Viability(OD:450nm)
Time(hours)
D
Ishikawa
shNC
shMETTL3
E
HEC-1B
F
HEC-1B
G
Ishikawa
HEC-1B
Migration
Migration cell numbers
H
Invasion
Invasion cell numbers
50μm

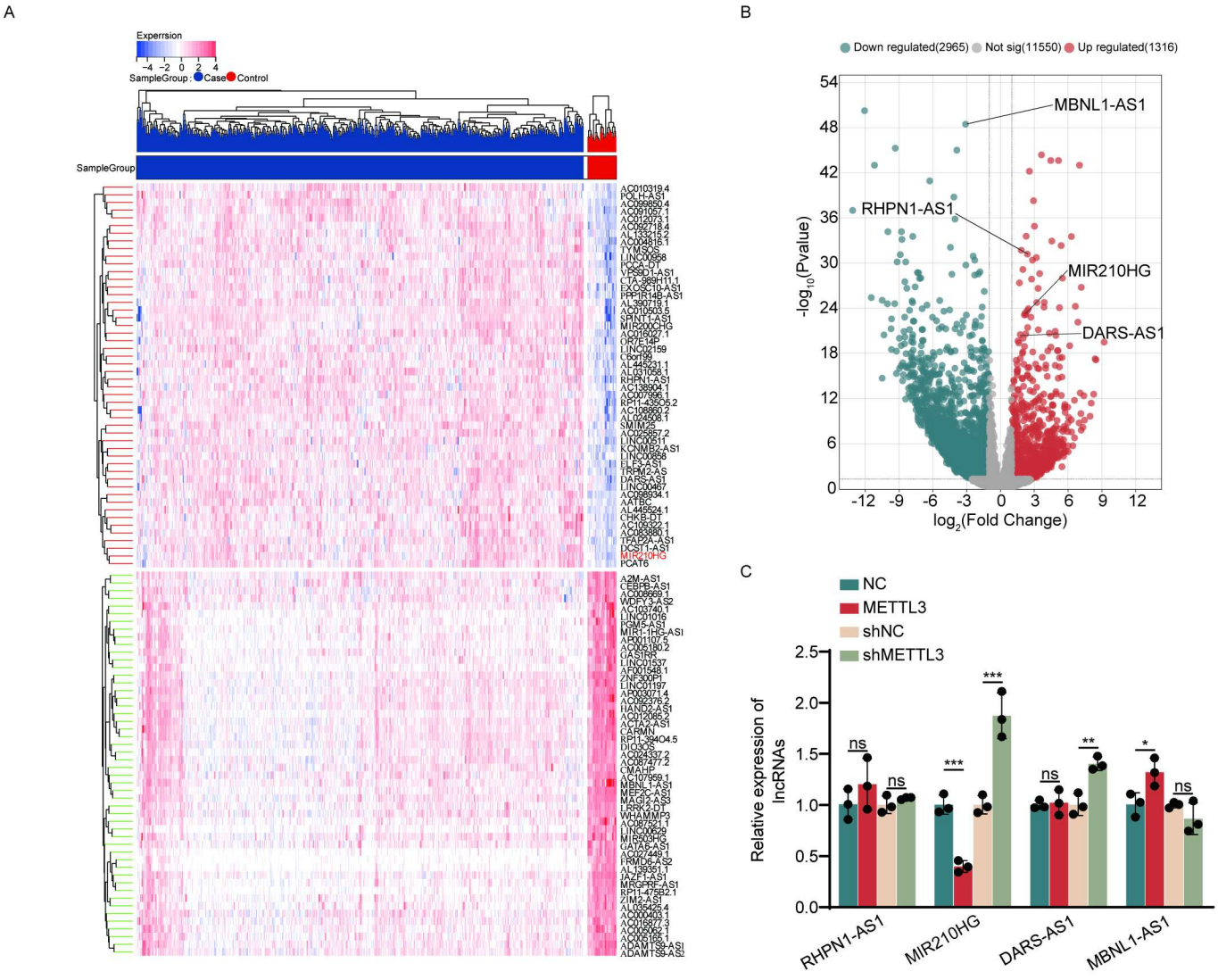
A
Experrsion
−4 −2 0 2 4
SampleGroup : Case Control
SampleGroup
B
Down regulated(2965) Not sig(11550) Up regulated(1316)
MBNL1-AS1
RHPN1-AS1
MIR210HG
DARS-AS1
-log10(Pvalue)
log2(Fold Change)
C
NC
METTL3
shNC
shMETTL3
Relative expression of lncRNAs
ns
***
**
*
RHPN1-AS1
MIR210HG
DARS-AS1
MBNL1-AS1

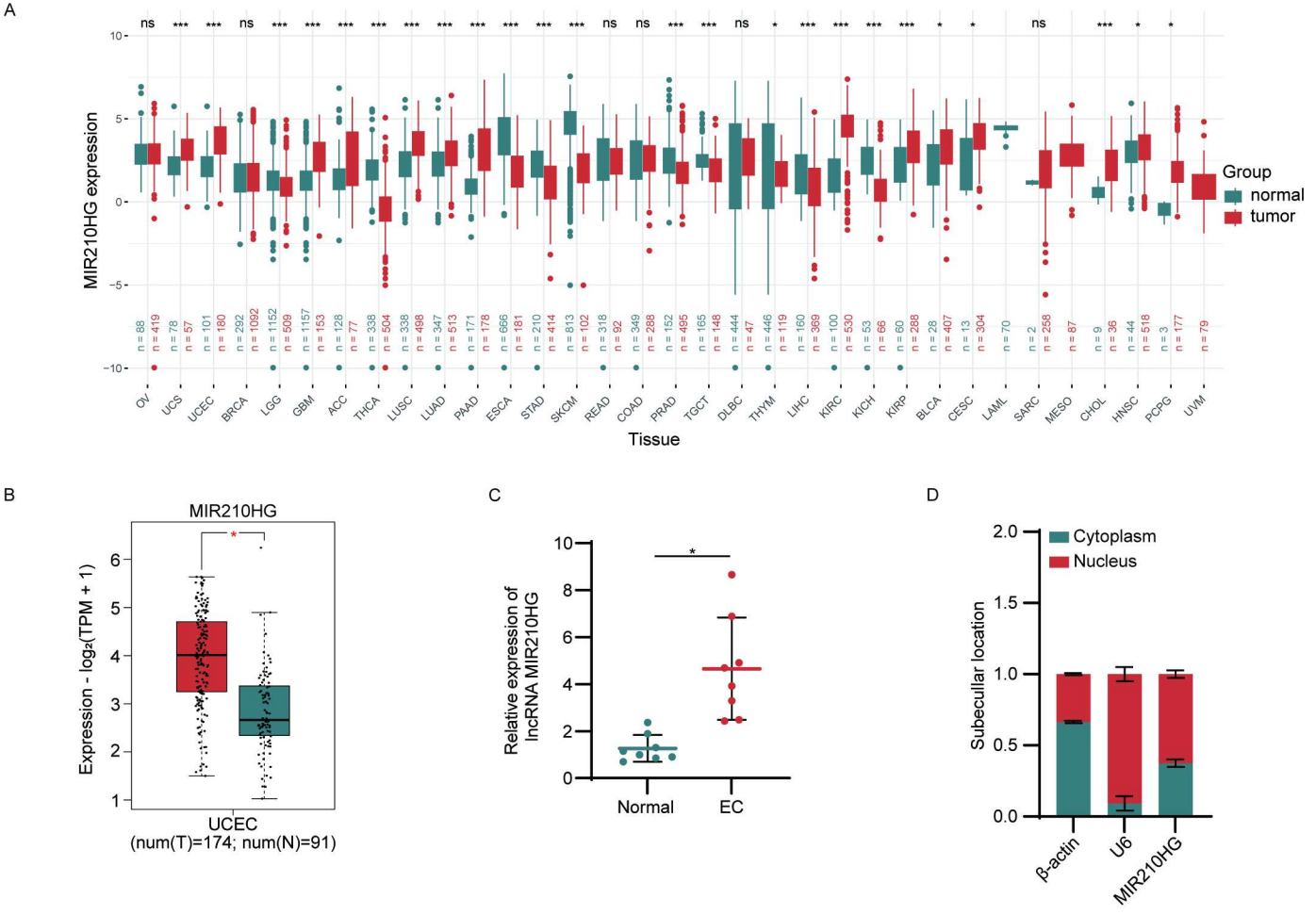
A
MIR210HG expression
Tissue
Group
normal
tumor
OV UCS UCEC BRCA LGG GBM ACC THCA LUSC LUAD PAAD ESCA STAD SKCM READ COAD PRAD TGCT DLBC THYM LIHC KIRC KICH KIRP BLCA CESC LAML SARC MESO CHOL HNSC PCPG UVM
B
MIR210HG
Expression - log2(TPM + 1)
UCEC
(num(T)=174; num(N)=91)
C
Relative expression of lncRNA MIR210HG
Normal
EC
D
Cytoplasm
Nucleus
Subecullar location
β-actin
U6
MIR210HG

A

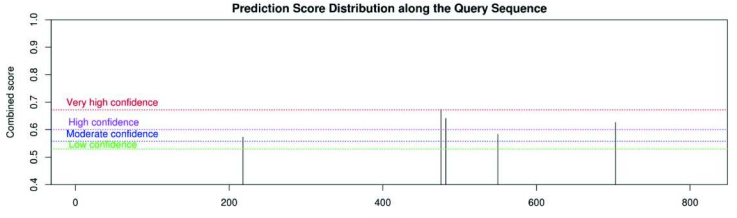

#	Position	Sequence context	Structural context	Local structure visualization	Score(binary)	Score(ann)	Score(spectrum)	Score(combined)	Decision
1	218	CUCCG GAGGG CCACC UCUGG GGACU UCCUA CGGGA AGAGA GUGAC	N/A	N/A	0.719	0.630	0.365	0.573	m^{6}A site (Moderate confidence)
2	476	AUUUA GUGGA CGCCU GGCAU GGACU CGGAC UGGCC UUUGG AAGCU	N/A	N/A	0.729	0.748	0.589	0.674	m^{6}A site (Very high confidence)
3	482	UGGAC GCCUG GCAUG GACUC GGACU GGCCU UUGGA AGCUC CCUGC	N/A	N/A	0.681	0.736	0.574	0.641	m^{6}A site (High confidence)
4	550	CUGCG AAGUG AGGCU UGGCA GGACC UGCAC CUGAG AAAGG CUGUG	N/A	N/A	0.516	0.663	0.665	0.583	m^{6}A site (Moderate confidence)
5	703	UCUGU GCUGG GGAUG AGUAG GAACU CUGGG CGAGG AGGGU CCCAG	N/A	N/A	0.638	0.612	0.612	0.626	m^{6}A site (High confidence)

B

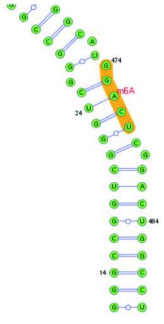

C

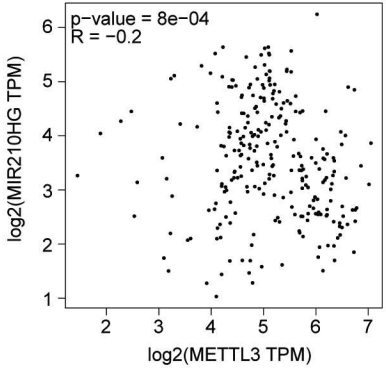

D

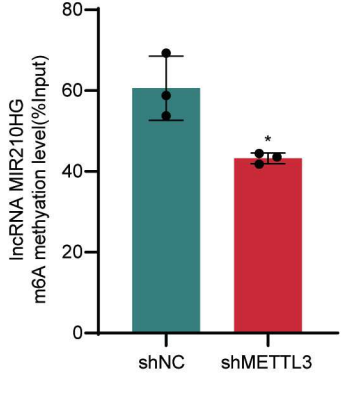

E

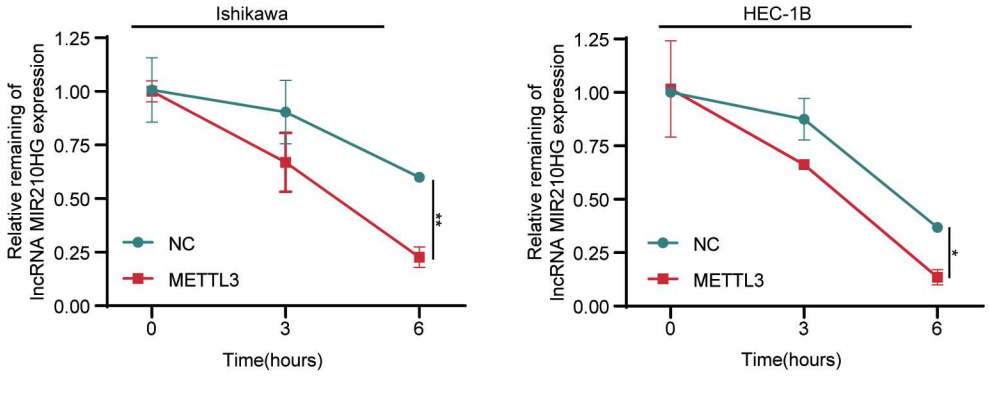

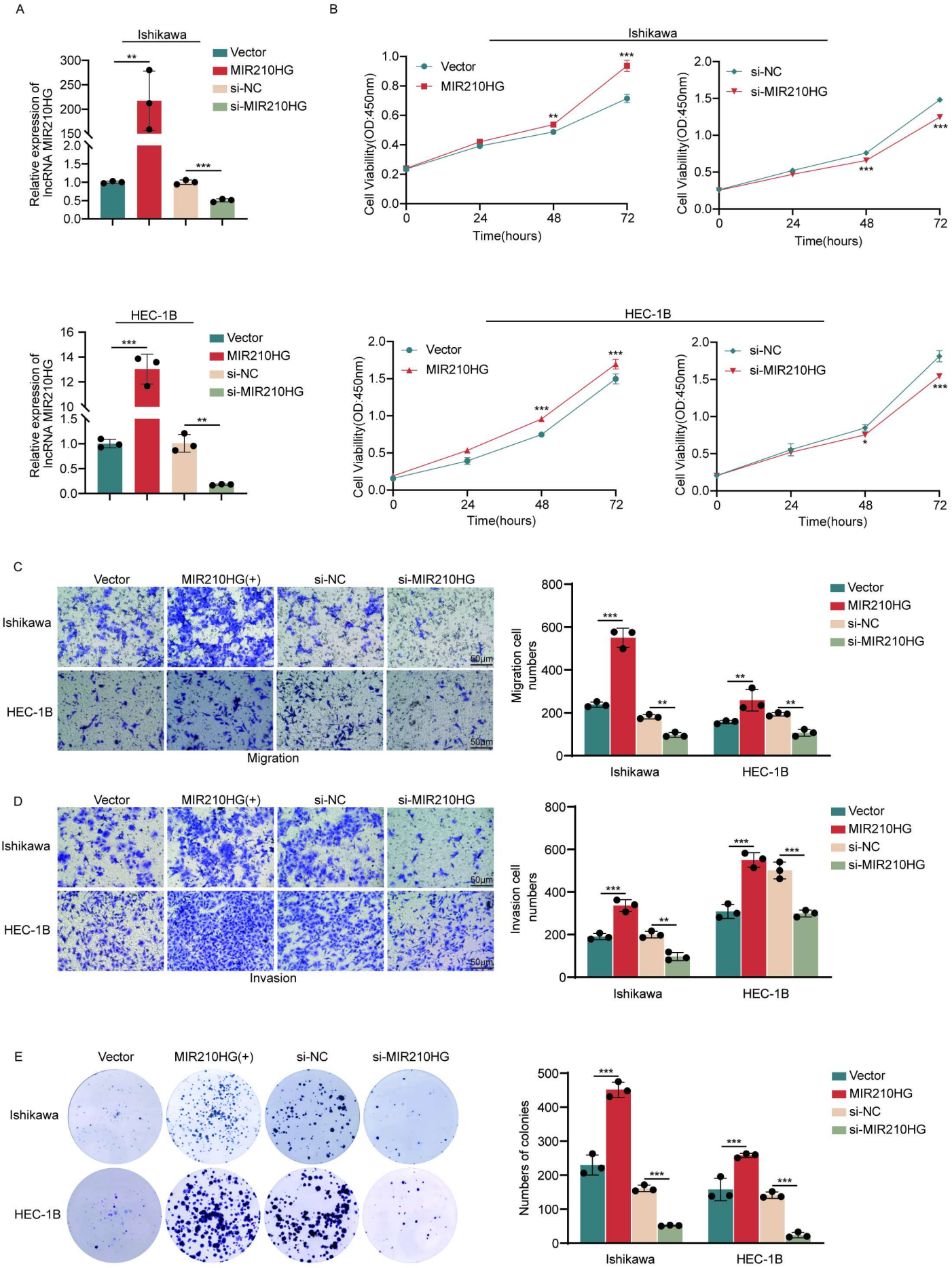
A
Ishikawa
Vector
MIR210HG
si-NC
si-MIR210HG
Relative expression of lncRNA MIR210HG
B
Ishikawa
Cell Viability(OD:450nm)
Time(hours)
HEC-1B
C
Vector
MIR210HG(+)
si-NC
si-MIR210HG
Migration
Migration cell numbers
D
Invasion
Invasion cell numbers
E
Numbers of colonies

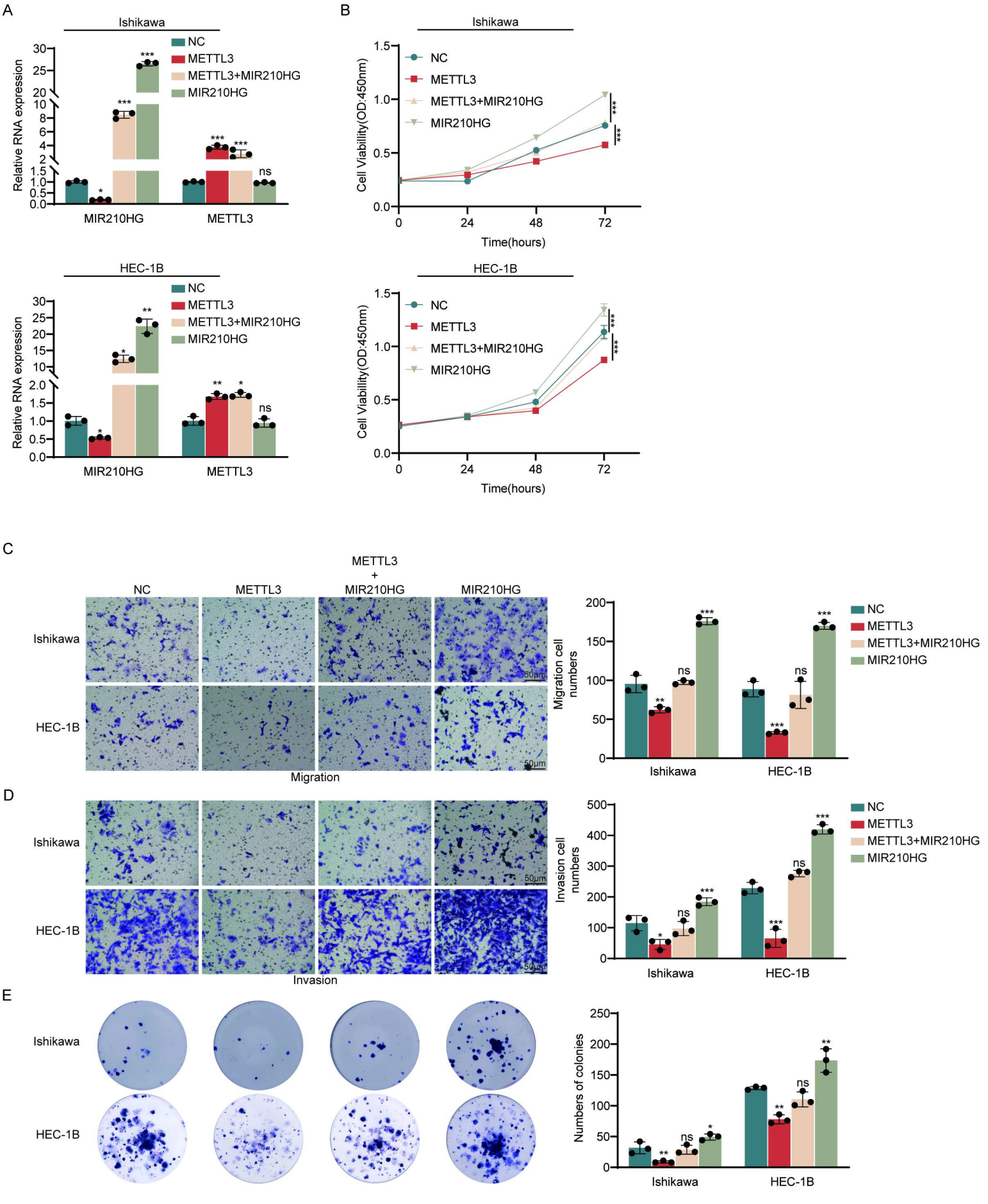
A
Ishikawa
NC
METTL3
METTL3+MIR210HG
MIR210HG
Relative RNA expression
MIR210HG
METTL3
HEC-1B
B
Ishikawa
Cell Viability(OD:450nm)
Time(hours)
HEC-1B
C
METTL3
+
MIR210HG
Migration
Migration cell numbers
D
Invasion
Invasion cell numbers
E
Numbers of colonies

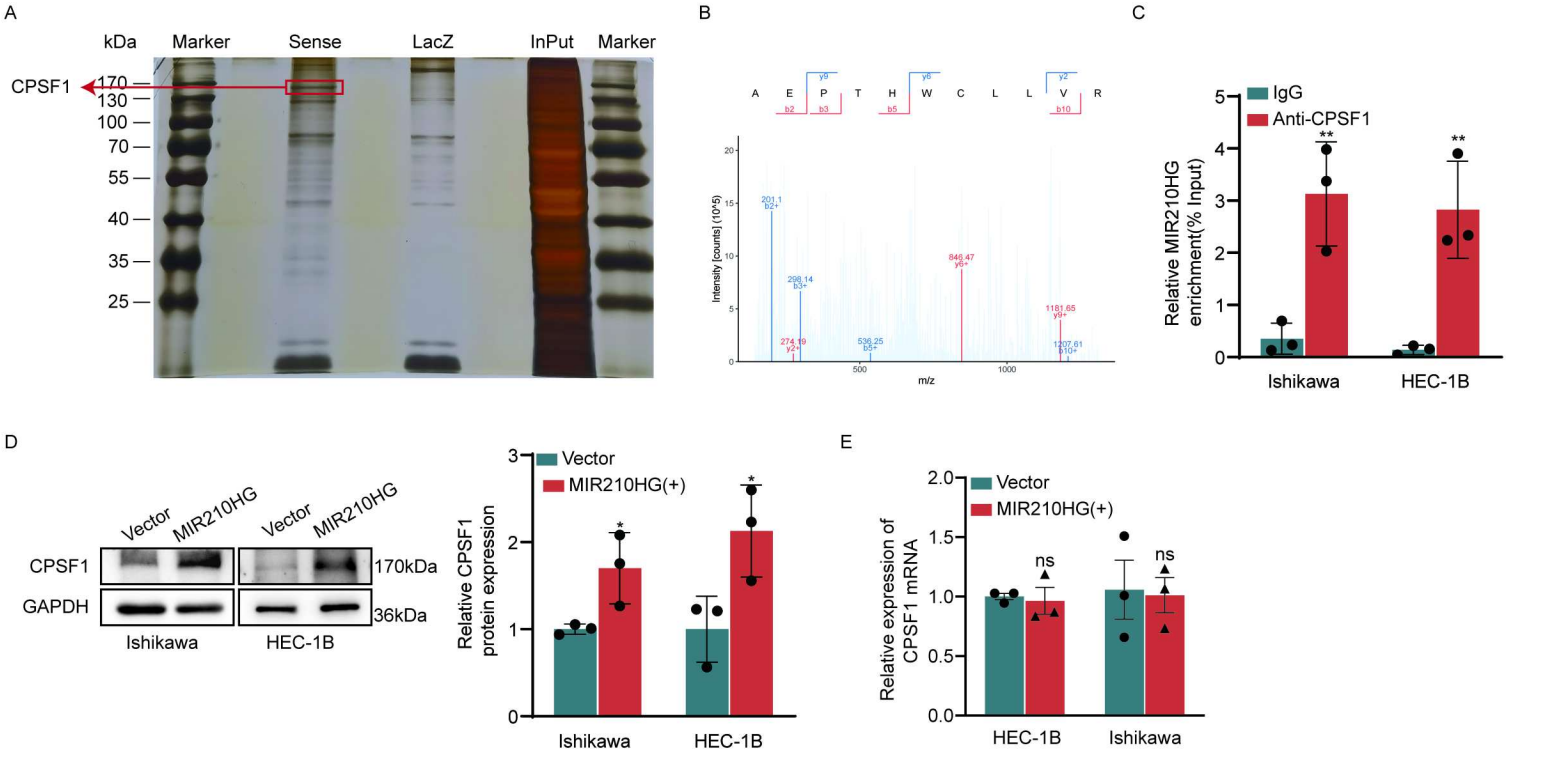
A
kDa
Marker
Sense
LacZ
InPut
Marker
CPSF1
170
130
100
70
55
40
35
25
B
A E P T H W C L L V R
b2 b3 b5 b10
y9 y6 y2
Intensity [counts] (10^5)
m/z
201.1
298.14
274.19
536.25
846.47
1181.65
1207.61
C
IgG
Anti-CPSF1
Relative MIR210HG enrichment(% Input)
Ishikawa
HEC-1B
D
Vector
MIR210HG
CPSF1
GAPDH
170kDa
36kDa
Ishikawa
HEC-1B
Relative CPSF1 protein expression
E
Relative expression of CPSF1 mRNA
ns

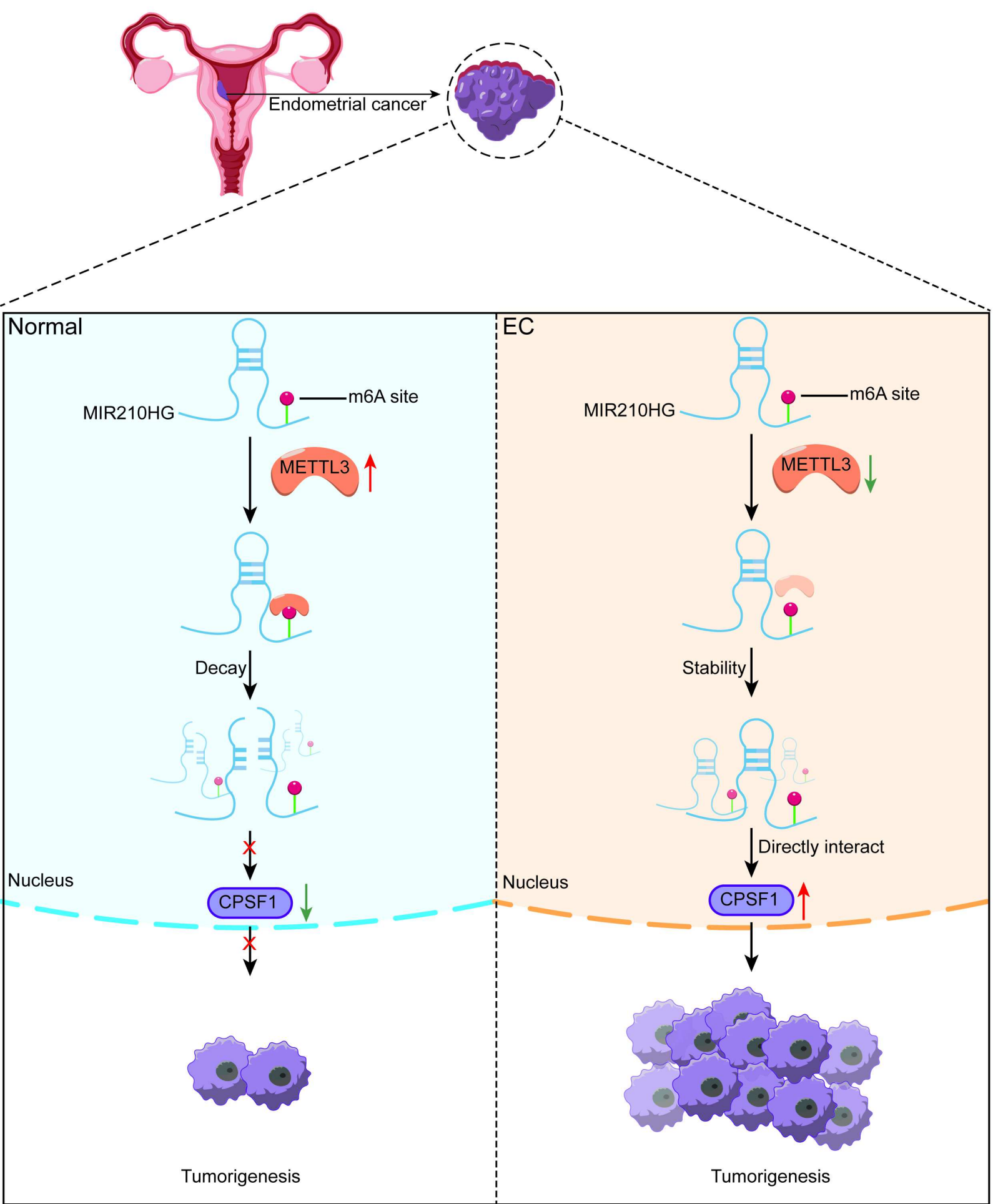
Endometrial cancer
Normal
MIR210HG
m6A site
METTL3
Decay
Nucleus
CPSF1
Tumorigenesis
EC
MIR210HG
m6A site
METTL3
Stability
Directly interact
Nucleus
CPSF1
Tumorigenesis

Supplementary Files

This is a list of supplementary files associated with this preprint. Click to download.

- Table2.docx
- Table3.docx
- Table1.docx